Published in final edited form as:
ACS ES T Eng. 2024 January 04; 4(2): 401–408. doi:10.1021/acsestengg.3c00365.

Engineered Electrically Heatable Face Masks for Direct Inactivation of Aerosolized Viruses on the Mask Surfaces

Hyunsik Kim,
Department of Chemical and Environmental Engineering, University of Cincinnati, Cincinnati, Ohio 45221, United States

Yanbo Fang,
Department of Mechanical and Materials Engineering, University of Cincinnati, Cincinnati, Ohio 45221, United States

Yoontaek Oh,
United States Environmental Protection Agency, Office of Research and Development, Cincinnati, Ohio 45268, United States; Pegasus Technical Services, Inc., Cincinnati, Ohio 45268, United States

Vesselin N. Shanov*,
Department of Chemical and Environmental Engineering, University of Cincinnati, Cincinnati, Ohio 45221, United States; Department of Mechanical and Materials Engineering, University of Cincinnati, Cincinnati, Ohio 45221, United States

Hodon Ryu*,
United States Environmental Protection Agency, Office of Research and Development, Cincinnati, Ohio 45268, United States

Soryong Chae*
Department of Chemical and Environmental Engineering, University of Cincinnati, Cincinnati, Ohio 45221, United States

Abstract

The COVID-19 pandemic has resulted in significant changes in our daily lives, including the widespread use of face masks. Face masks have been reported to reduce the transmission of

Corresponding Authors Vesselin N. Shanov — Department of Chemical and Environmental Engineering, University of Cincinnati, Cincinnati, Ohio 45221, United States; Department of Mechanical and Materials Engineering, University of Cincinnati, Cincinnati, Ohio 45221, United States; shanovvn@ucmail.uc.edu; **Hodon Ryu** — United States Environmental Protection Agency, Office of Research and Development, Cincinnati, Ohio 45268, United States; ryu.hodon@epa.gov; **Soryong Chae** — Department of Chemical and Environmental Engineering, University of Cincinnati, Cincinnati, Ohio 45221, United States; chaesg@ucmail.uc.edu.

Author Contributions

CRediT: **Hyunsik Kim** formal analysis, investigation, writing-original draft; **Yanbo Fang** investigation; **Yoontaek Oh** methodology, writing-original draft; **Vesselin Shanov** supervision, writing-review & editing; **Hodon Ryu** supervision, writing-review & editing; **Soryong Chae** supervision, writing-original draft, writing-review & editing.

Supporting Information

The Supporting Information is available free of charge at https://pubs.acs.org/doi/10.1021/acsestengg.3c00365.

Inactivation of virus at various Joule heating temperatures; inactivation of virus at various Joule heating times; fabrication procedures of an electrically heatable carbon veil layer; pressure drop measurement system; Joule heating performance of a CNT sheet; pressure drops of ASTM Level 3 masks with Joule heating (PDF)

The authors declare no competing financial interest.

viral infections by droplets; however, improper use and/or treatment of these masks can cause them to be contaminated, thereby reducing their efficacy. Moreover, regular replacement of face masks is essential to maintaining their effectiveness, which can be challenging in resource-limited healthcare settings. The initial scarcity of face masks during the early stages of the pandemic led to the development of reusable face mask solutions. This research aimed to design a porous, standalone electrically heatable carbon veil (CV) layer that can be applied to commercial face masks without compromising their breathability. The main objective of this study is to directly inactivate aerosolized viruses using CV heaters powered by a direct current (DC). Prototype face mask samples with the CV were produced and tested using the aerosolized MS2 bacteriophage. After contamination of the face mask with the MS2 bacteriophage, the mask was treated by applying a direct current of 6 V and 1.17 A, which caused the surface temperature of the CV layers to reach over 70 °C within 10 s. This rapid temperature increase through Joule heating effectively inactivates the captured MS2 bacteriophage, with an average inactivation efficiency exceeding 99%. The findings of this study provide valuable insights into the potential application of engineered carbon layers for the decontamination of face masks and air filters from aerosolized viruses, thereby potentially enabling their reuse.

Graphical Abstract

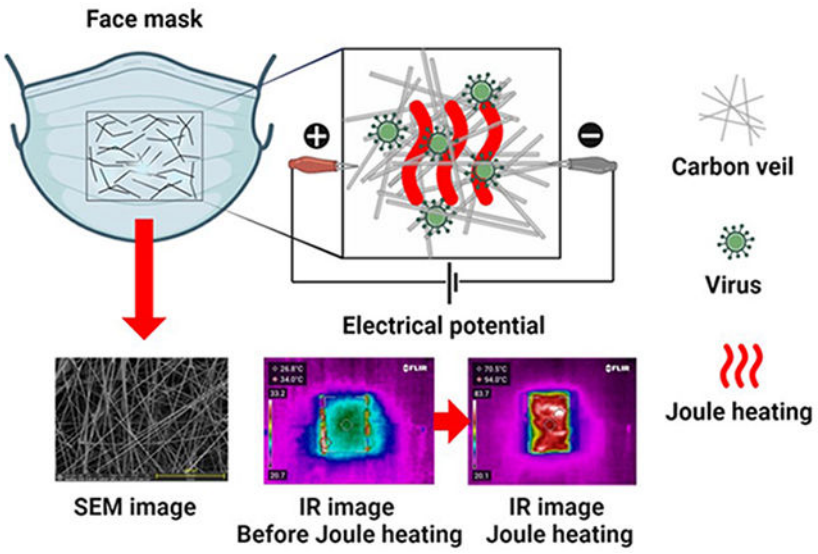

Keywords

reusable face mask; electrically heatable carbon veil layer; direct inactivation; aerosolized MS2 bacteriophage; Joule heating

1. INTRODUCTION

The COVID-19 (SARS-CoV-2) pandemic has had a profound impact on human life, necessitating widespread adoption of face masks as a preventive measure. Viruses, including SARS-CoV-2, can be transmitted through various means such as direct contact, respiratory droplets, and aerosol.[1-3]

Numerous studies have investigated the effectiveness of wearing masks in reducing the transmission of viruses.[3,4] Masks serve as physical barriers that help protect users from potential virus exposure.[5] More specifically, the filtration performance of face masks is primarily attributed to the presence of electrostatically charged nonwoven fibers. Coulombic forces attract positively and negatively charged particles, while neutral particles can be polarized and subsequently captured by a bipolar electric field created by the reverse-charged layers of face masks.[6]

The high demand for face masks has led to shortages[7-9] and has exposed vulnerabilities in the supply chain for face masks,[10] further exacerbating the COVID-19 pandemic situation. Moreover, the extensive use of face masks has resulted in increased plastic waste, primarily composed of materials such as polypropylene (PP), polyethylene terephthalate (PET), and polyethylene (PE).[11-13]

This surge in plastic waste has become a new environmental concern. In addition, used masks may contain potentially infectious materials, posing a risk to public health and safety by increasing the potential for exposure to infectious viruses.[14,15] Thus, these factors have driven the urgent need for the mass production of both single-use and reusable masks as well as the development of effective decontamination methods for used masks.

Existing literature has extensively focused on conducting comprehensive experiments to develop reusable face masks, explore various decontamination methods, and assess their effects on masks granted emergency use authorization (EUA) for safe reutilization. Various approaches have been investigated, including steam treatment,[16-20] heat treatment,[18,20-24] ultraviolet (UV) irradtion,[17,18,22,25] chemical treatments (e.g., hydrogen peroxide, ethanol, and chlorine-based solutions)[17,18,22], and others (microwave, hot water, ozone).[17,26,27]

Steam treatment is widely recognized for its efficacy in face mask decontamination. Ma et al. conducted decontamination experiments on face masks using avian infectious bronchitis virus H120 and found that subjecting the masks to steam treatment through boiling water for 5 min led to complete inactivation of the avian viruses.[16] He et al. reported that steam treatment within the temperature range of 90–100 °C for durations of 30 and 90 min, respectively, resulted in complete inactivation of *Escherichia coli* and *Bacillus subtilis*, demonstrating greater than 4 log-reductions.[17]

UV irradiation, particularly using short-wave ultraviolet-C (UV–C), is another established decontamination method applied to various mediums. UV–C functions as a germicidal agent, causing damage to the deoxyribonucleic acid (DNA) of microorganisms and rendering them nonviable.[28] A recent study demonstrated that UV irradiation at a dosage of 0.12 J/cm^2 could achieve nearly 100% inactivation for *E. coli.*[17] Furthermore, a separate investigation focused on the decontamination of N95 masks contaminated with H1N1 influenza. It revealed a significant log reduction (≥3 log) between the contaminated and treated N95 masks, achieved through UV irradiation at 1.1 J/cm^2.[29]

Hydrogen peroxide (H_2O_2) was employed to assess the effectiveness of viral inactivation on face masks. Research revealed that vaporized H_2O_2, utilizing a 59% liquid concentration, proved effective in decontaminating porcine respiratory coronavirus (PRCV) from

contaminated masks, resulting in a reduction in viral infectivity by more than 3 orders of magnitude.[30]

Nevertheless, steam treatment, UV irradiation, and chemical treatments demand specialized equipment for disinfection and might result in the generation of hazardous chemical waste. In response to the challenges presented by current face mask decontamination methods, a novel approach has been developed, incorporating electrically heatable carbon nanotube (CNT) films onto filter surfaces. This innovative technology has demonstrated significant efficacy in disinfecting microorganisms, as observed in prior studies,[31,32] and showcasing remarkable efficiency in deactivating waterborne bacteria such as *Escherichia coli* (99%) and *Legionella pneumophila* (>99.99%). However, scaling the manufacturing of electrically heatable masks without the use of expensive CNT material that can satisfy the requirements for mass production of a carbon-based, breathable, lightweight, and flexible heater is currently uncertain.

In our initial tests, applying CNT layers to the surface of ASTM Level 3 face masks resulted in a significant increase in airflow resistance, compromising the masks' breathability. Specifically, the airflow resistance measured in our preliminary tests exceeded the standard limit of 58.8 Pa/cm^2 for the ASTM Level 3 masks (unpublished data).

To address concerns related to CNT layer breathability, we have developed a porous and freestanding heating layer using a commercialized carbon veil (CV). The CV layer possesses electrical heating capabilities and is specifically designed for inactivating viruses that may adhere to face masks. The objective is to investigate whether the CV layer can provide effective viral inactivation without significantly compromising the breathability and the generation of (bio)chemical waste.

The surface morphology, electrothermal properties, and breathability performance of the CV heater were comprehensively analyzed. Subsequently, the CV layer has been integrated into commercial face masks, and the electrical heating capability of the CV layer has been assessed for its effectiveness in inactivating airborne pathogens using a surrogate virus.

This study involves designing and fabricating heatable and reusable face mask samples that can capture and neutralize aerosolized viruses present on mask surfaces, thus preventing their entry into the human respiratory system. This is achieved through resistive heating, raising the temperature above the virus's lethal threshold, approximately 70 °C.[33] A thin and breathable CV heater can be retrofitted or applied to the outer surface of any commercial face mask to facilitate resistive heating.

2. EXPERIMENTAL SECTION

2.1. Face Mask and the CV Layer.

The base material for this study comprised commercial ASTM Level 3 face masks (Vaxxen Laboratories, USA). CV and face mask composites were manufactured using a commercialized CV (ACP Composites, USA), which contained chopped carbon fibers and utilized a nonwoven process with a small amount of polyester (refer to Table 1).

2.2. Engineering Design of an Electrically Heatable Face Masks.

An electrically heatable CV was combined with commercial face masks after a simple modification process (Figure S1). First, the CV layer was cut into 7.5 cm by 7.5 cm section. Acetone (>99.5%, Alfa Aesar) was then employed to remove the polymeric binders present in the CV sheet. Cu foils (0.15 mm thickness, 1 cm × 7.5 cm, Yodaoke, China) were attached to the CV layer using conductive silver paint (Ted Pella, Inc.), then copper wire was soldered onto each copper foil. Lastly, the engineered CV layer, with an active heating area measuring 5.5 cm by 7.5 cm, was positioned on the outer layer of commercial face masks for subsequent testing.

2.3. Characterization of Electrically Heatable Face Masks.

2.3.1. Breathability Test.—To assess the airflow resistance caused by the CV layer, the pressure drops of face masks coupled with the CV layer were measured using a vacuum pressure system in accordance with ASTM F2100-19 and EN 14683:2019 standards, as illustrated in Figure S2a. The vacuum pressure system comprises a digital manometer (475-2-FM, Dwyer), a sample holder (KF25, Advantech), and a mass flow controller (MCR-100 SLPM, Alicat Scientific).

The components of the sample holder are depicted in Figure S2b. Coupons of face masks, CV sheets, or CV/face mask composites with diameters of 2.54 cm were prepared to fit the sample holder with an effective surface area of 3.8 cm^2. The breathability procedures outlined in EN 14683:2019 suggest using a velocity of approximately 1632.7 cm/min (equivalent to 8 L/min airflow) with an effective area of 4.9 cm^2 for the sample holder. To ensure consistency with the specified effective area of 3.8 cm^2 for our setup, the airflow was maintained at 6.2 L/min throughout all breathability tests, aligning with the prescribed velocity. The net pressure drop of the test samples was calculated by subtracting the pressure drop of the sample holder (i.e., control) from the total pressure drop of the sample holder with the test samples. The net pressure drop was then normalized by the effective area in accordance with ASTM standard.

2.3.2. Surface Morphologies and Elemental Analysis of Electrically Heatable Face Masks.—A scanning electron microscope (SEM) (APREO C, ThermoFisher) equipped with energy dispersive X-ray analysis (EDX) was used to examine the surface morphologies and the elemental composition of the face masks and CV sheets. Prior to SEM analysis, the samples were sputter-coated using a Desk V coating system (Desk V, Denton Vacuum).

2.4. Direct Inactivation of Airborne Virus Surrogate on the Face Masks.

2.4.1. Preparation of a Virus Surrogate Suspension.—A stock suspension of the MS2 bacteriophage, which served as a virus surrogate, was prepared as follows: Stock MS2 bacteriophage (ATCC 15597-B1) was added to 30 mL of tryptic soy broth (TSB) (Fisher Scientific). The bacteriophage suspension was then aseptically combined with 6 mL of a mid log growth phase *E. coli* F_{amp} culture (ATCC 700891) and 90 mL of 0.7% tryptic soy agar (TSA) (Fisher Scientific) supplemented with antibiotics (0.015 mg each streptomycin and ampicillin per ml of agar for *E. coli* F_{amp}). The mixture was thoroughly mixed, and

then 6 mL was overlaid onto 1.5% TSA supplemented with the same antibiotics in 100 mm plates. After the top agar set, the plates were incubated at 37 ± 0.5 °C for 24 h. The MS2 bacteriophages were harvested by adding 5 mL of TSB to each plate and incubating at room temperature for 2 h. The plates were then swirled 20 times, and the broth from all of the agar plates was combined into a sterile 50 mL tube. The broth was centrifuged at 3000*g* for 5 min, and the supernatant was sterilized using a 0.2 μm filter. The clarified supernatant was decanted in sterile containers and stored at 4 °C before use.

2.4.2. Aerosolization and Filtration of Airborne Virus Surrogate.—A system was set up to generate and capture aerosolized MS2 onto face masks, as shown in Figure 1. Prior to the tests, the MS2 bacteriophage stock was diluted to a working concentration of approximately 1×10^9 PFU/mL. A test sample coupon with a diameter of 4.3 cm was placed on the sample holder, which was then connected to a commercial nebulizer (YS35, Meowyn). To generate aerosolized MS2, 8 mL of the diluted MS2 stock suspension was loaded into the nebulizer. The aerosolized MS2 was then captured onto face mask samples using vacuum suction at a flow rate of about 18 L/min. Once the capture of aerosolized MS2 onto the test sample coupon was complete, the coupon was collected and dried for 2 h on a glass plate at room temperature in ambient air.

2.4.3. Joule Heating of the CV Heater.—Joule heating of the CV sheet was conducted by using DC power. A DC power supply (9111, BK precision) was used to provide electrical power to the 5.5 × 7.5 cm CV layer. The electrical power was controlled based on voltage, and the surface temperature of the CV layer and electrical current were monitored as the voltage increased. The performance of the prepared CV layer was evaluated by measuring the surface temperature of the CV layer by using an IR camera (C5, FLIR). After the Joule heating process, the two electrodes were removed from the CV layer. The electrically heated sample was then transferred into a 50 mL conical tube containing 20 mL of Butterfield's buffer solution. The sample was vortexed for one min to recover the MS2 bacteriophage from the test sample.

2.4.4. Virus Assay.—The recovered MS2 bacteriophages from the test samples were serially diluted and enumerated in duplicate following EPA Method 1601 (USEPA, 2001). To confirm the enumeration, 1 mL of each dilution using TSB was added to 3 mL of soft top agar consisting of 0.75% TSA containing the mid log growth phase host bacteria. The inoculated top agar was then poured over a 1.5% TSA bottom agar plate and allowed to solidify. The plates were inverted and incubated at 37 ± 0.5 °C for 16 to 24 h. The viral plaques formed on the plates were counted to determine the concentration of coliphage.

The log inactivation value (I) of the MS2 bacteriophage is defined by the following equation:

$$\text{Log inactivation value, } I = -\log_{10}\left(\frac{N}{N_0}\right)$$

where N is the MS2 bacteriophage concentration (PFU/mL) after Joule heating and N_0 is the MS2 bacteriophage concentration (PFU/mL) before Joule heating.

2.5. Statistical Analysis.

A basic statistical analysis was conducted employing a one-way analysis of variance (ANOVA) using Microsoft Excel. The surface temperature of CV and Joule heating time of CV were treated as individual variables to analyze their respective impacts on MS2 inactivation. A statistical significance level of $\alpha = 0.05$ was established. The study's ANOVA design will be elaborated upon in section 3.3.

3. RESULTS AND DISCUSSION

3.1. Characteristics of Electrically Heatable Face Masks.

Figure 2a shows the schematic diagram of an electrically heatable face mask with a CV layer on the mask outer surface. SEM images reveal that the CV layer exhibits a nonwoven structure with stacked carbon fibers (Figure 2b). Typical disposable masks comprise two outer layers, usually spun-bond polypropylene (depicted as the top and bottom layers in Figure 2a), and a melt-blown layer (the middle layer in Figure 2a), primarily composed of polypropylene.[34-36] All layers of the face masks are composed of nonwoven fabric (Figure 2c-e). The filter layer, situated in the middle layer, shows a denser surface morphology (Figure 2d) compared to the top and bottom layers (Figure 2c and e). EDX analysis confirmed the presence of carbon (C) and smaller amounts of oxygen (O) on the CV layer (Figure 2f).

Pressure drop measurements were performed on randomly selected mask samples. The normalized net pressure drop was calculated considering the effective area of mask coupons (i.e., 3.8 cm^2). The breathability tests revealed that the normalized net pressure drop for the commercial ASTM Level 3 mask and the mask coupled with the CV layer were determined to be 46.8 ± 2.86 and 48.1 ± 3.30 Pa/cm^2, respectively. These results indicate that the additional CV layer does not compromise the breathability performance of commercial ASTM Level 3 masks, as depicted in Figure 3. This is further supported by the measurement of the net pressure drop of the free-standing CV layer, which was determined to be 0.1 ± 0.03 Pa/cm^2 (Table 1).

3.2. Joule Heating Performance for the Electrically Heatable CV Layer.

An electrically heatable CV layer was positioned on a thermally insulated plate (Figure 4a), and the surface temperature of the CV layer was measured using an IR camera (Figure 4b and c). By applying DC power to the CV layer in air, heat was generated on the surface (Figure 4d). The average surface temperature (averaged over 60 s) of the CV layer ranged from 26.9 ± 0.19 to 105.7 ± 0.94 °C, with an increase in the applied DC power from 0.2 to 11.9 W. It is noteworthy that the surface temperature of the CV layer exhibited a proportional relationship with the applied power, following Joule's law (Figure 4e). Similar observations have been reported for other carbon-based materials and metals.[37,38] Joule heating performance of a CNT sheet was demonstrated in Figure S3.

3.3. Direct Inactivation of MS2 on an ASTM Level 3 Mask Using Joule Heating.

To investigate the inactivation of MS2, direct inactivation tests were conducted by using Joule heating at various surface temperatures and heating times. Figure 5 represents the

log-concentrations of active MS2 in the control (without Joule heating) and thermally treated samples using Joule heating at three different temperatures for 5 min. The log-concentrations of active MS2 are as follows: 7.0 ± 0.10 (control), 3.8 ± 0.63 (joule heating at 70 °C), 4.9 ± 0.04 (joule heating at 80 °C), and 4.3 ± 0.02 (joule heating at 90 °C). It is evident that the highest inactivation efficiency occurred with Joule heating at 70 °C for 5 min, resulting in an inactivation efficiency of 3.2 ± 0.72 (Table S1).

The effects of different heating times on the inactivation efficiency were also investigated. Joule heating was performed at 70 °C for different durations, ranging from 5 to 15 min. The log-concentrations of active MS2 under different conditions are as follows: 6.9 ± 0.76 (control), 3.3 ± 0.85 (Joule heating for 5 min), 4.2 ± 0.85 (Joule heating for 10 min), and 3.4 ± 1.90 (Joule heating for 15 min) (Figure 6).

The experimental results demonstrate that there is no significant difference in the MS2 inactivation efficiency as the heating time is increased during Joule heating. Regardless of the heating time, the MS2 inactivation efficiency was greater than 99% in all conditions (Table S2). This can be attributed to the rapid increase in the surface temperature of the CV layer from room temperature to the targeted temperature levels (as shown in Figure 4d), allowing for the efficient inactivation of most of the captured MS2 on the ASTM Level 3 masks within a few minutes.

Considering the experimental conditions outlined in this section, one-way ANOVAs were performed to assess variations in two parameters: (1) surface temperature of CV ranging from 70 to 90 °C and (2) heating time ranging from 5 to 15 min. The results of statistical analysis indicate that increased heating time (5–15 min) and surface temperatures (70–90 °C) resulting from Joule heating do not have a statistically significant effect on the inactivation of captured MS2. This conclusion is drawn by rejecting the null hypothesis, which suggests a correlation between heating time, the surface temperatures, and the efficiency of MS2 inactivation. The obtained p-values for heating time and surface temperatures are 0.29 and 0.54, respectively.

To account for these unexpected findings, it is hypothesized that the surface roughness and the porous nature of the top layer of masks (depicted in Figure 2c) could potentially impede the dissipation of heat from the CV heaters to the middle layer (as shown in Figure 2d). This limitation may arise due to the relatively low thermal conductivity of the air trapped in the middle layer.

In terms of the reusability of face masks, it has been reported that steam decontamination can lead to the degradation of the static charge in the fibers, resulting in a substantial reduction of its filtration efficiency. For instance, Liao et al. observed that the efficiency of melt-blown material decreased from 96.5% to 85% after 5 cycles of decontamination using boiled water-assisted steam treatment for 10 min.[18] Similarly, UV irradiation has the potential to cause material damage in face masks.[18,39] Furthermore, careful consideration of face mask design is necessary when implementing UV irradiation, as mask materials can absorb UV light, possibly leading to inadequate disinfection.[18,29,40,41]

To investigate the reusability of face masks equipped with CV heaters, we conducted pressure drop measurements during Joule heating using a custom-designed sample holder. Our observations revealed a significant increase in normalized net pressure drop, ranging from 69.2 to 77.4 Pa/cm^2 (before Joule heating) to 108.9 to 118.9 Pa/cm^2 (at a surface temperature of 65 °C with Joule heating), as depicted in Figure S4. This rise can be attributed to the expansion of air when passing through the heated CV layer. Notably, the normalized net pressure drop could be restored to its initial value upon discontinuing Joule heating. This indicates that no structural deformation of the face masks is expected because of Joule heating.

4. CONCLUSIONS

In this study, we developed and integrated a porous, electrically heatable layer into a face mask material using commercial CV to effectively inactivate aerosolized MS2 bacteriophages. The results unequivocally demonstrate that the electrically heatable CV material preserved the breathability performance of the commercially available ASTM Level 3 mask. Moreover, through the utilization of Joule heating facilitated by the CV heater, we successfully achieved the inactivation of MS2 particles that were captured on the masks. This process resulted in an average inactivation efficiency exceeding 99.9% at 70 °C, which represents approximately a 3.2–3.6-log reduction in MS2 viability. This outcome was attained using approximately 2.1 kJ of energy, necessary to initiate Joule heating and raise the surface temperature of the masks to 70 °C for a duration of 5 min. To further enhance the efficiency of inactivation, potential improvements lie in optimizing the design of the interface between CV and face masks. These findings underscore the potential of utilizing Joule heating via an electrically conductive CV material for decontamination and the potential reutilization of used masks.

Supplementary Material

Refer to Web version on PubMed Central for supplementary material.

ACKNOWLEDGMENTS

This study was supported by the National Science Foundation (NSF) (Award number: CBET 2028625). The information in this article has been reviewed in accordance with the U.S. Environmental Protection Agency's (EPA's) policy and approved for publication. The views expressed in this article are those of the authors and do not necessarily represent the views or the policies of EPA. Any mention of trade names, manufacturers, or products does not imply an endorsement by the U.S. Government or EPA; EPA and its employees do not endorse any commercial products, services, or enterprises.

REFERENCES

(1). Richard M; Kok A; De Meulder D; Bestebroer TM; Lamers MM; Okba NMA; Fentener Van Vlissingen M; Rockx B; Haagmans BL; Koopmans MPG; Fouchier RAM; Herfst S SARS-CoV-2 is transmitted via contact and via the air between ferrets. Nat. Commun 2020, 11, 3496. [PubMed: 32641684]

(2). Liu Y; Ning Z; Chen Y; Guo M; Liu Y; Gali NK; Sun L; Duan Y; Cai J; Westerdahl D; Liu X; Xu K; Ho K-F; Kan H; Fu Q; Lan K Aerodynamic analysis of SARS-CoV-2 in two Wuhan hospitals. Nature 2020, 582 (7813), 557–560. [PubMed: 32340022]

(3). Bundgaard H; Bundgaard JS; Raaschou-Pedersen DET; von Buchwald C; Todsen T; Norsk JB; Pries-Heje MM; Vissing CR; Nielsen PB; Winsløw UC; et al. Effectiveness of adding a mask recommendation to other public health measures to prevent SARS-CoV-2 infection in Danish mask wearers: a randomized controlled trial. Annals of internal medicine 2021, 174 (3), 335–343. [PubMed: 33205991]

(4). Brooks JT; Butler JC Effectiveness of mask wearing to control community spread of SARS-CoV-2. Jama 2021, 325 (10), 998–999. [PubMed: 33566056]

(5). Chua MH; Cheng W; Goh SS; Kong J; Li B; Lim JYC; Mao L; Wang S; Xue K; Yang L; Ye E; Zhang K; Cheong WCD; Tan BH; Li Z; Tan BH; Loh XJ Face Masks in the New COVID-19 Normal: Materials, Testing, and Perspectives. Research 2020, 2020, 1–40.

(6). Tsai P. Performance of masks and discussion of the inactivation of SARS-CoV-2. Engineered Science 2020, 10 (5), 1–7.

(7). Worby CJ; Chang H-H Face mask use in the general population and optimal resource allocation during the COVID-19 pandemic. Nat. Commun 2020, 11, 4049. [PubMed: 32792562]

(8). Wang M; Zhou M; Ji G; Ye L; Cheng Y; Feng Z; Chen J Mask crisis during the COVID-19 outbreak. Eur. Rev. Med. Pharmacol Sci 2020, 24 (6), 3397–3399. [PubMed: 32271457]

(9). Feng S; Shen C; Xia N; Song W; Fan M; Cowling BJ Rational use of face masks in the COVID-19 pandemic. Lancet Respiratory Medicine 2020, 8 (5), 434–436. [PubMed: 32203710]

(10). Armani AM; Hurt DE; Hwang D; McCarthy MC; Scholtz A Low-tech solutions for the COVID-19 supply chain crisis. Nature Reviews Materials 2020, 5 (6), 403–406.

(11). Patrício Silva AL; Prata JC; Walker TR; Duarte AC; Ouyang W; Barcelò D; Rocha-Santos T Increased plastic pollution due to COVID-19 pandemic: Challenges and recommendations. Chemical Engineering Journal 2021, 405, No. 126683. [PubMed: 32834764]

(12). Ajmeri J; Ajmeri CJ Nonwoven materials and technologies for medical applications. In Handbook of medical textiles; Elsevier: 2011; pp 106–131.

(13). Selvaranjan K; Navaratnam S; Rajeev P; Ravintherakumaran N Environmental challenges induced by extensive use of face masks during COVID-19: A review and potential solutions. Environmental Challenges 2021, 3, No. 100039. [PubMed: 38620606]

(14). Benson NU; Bassey DE; Palanisami T COVID pollution: impact of COVID-19 pandemic on global plastic waste footprint. Heliyon 2021, 7 (2), No. e06343. [PubMed: 33655084]

(15). Chin AW; Chu JT; Perera MR; Hui KP; Yen H-L; Chan MC; Peiris M; Poon LL Stability of SARS-CoV-2 in different environmental conditions. Lancet Microbe 2020, 1 (1), No. e10. [PubMed: 32835322]

(16). Ma QX; Shan H; Zhang CM; Zhang HL; Li GM; Yang RM; Chen JM Decontamination of face masks with steam for mask reuse in fighting the pandemic COVID-19: experimental supports. Journal of medical virology 2020, 92 (10), 1971–1974. [PubMed: 32320083]

(17). He W; Guo Y; Gao H; Liu J; Yue Y; Wang J Evaluation of Regeneration Processes for Filtering Facepiece Respirators in Terms of the Bacteria Inactivation Efficiency and Influences on Filtration Performance. ACS Nano 2020, 14 (10), 13161–13171. [PubMed: 32975412]

(18). Liao L; Xiao W; Zhao M; Yu X; Wang H; Wang Q; Chu S; Cui Y Can N95 Respirators Be Reused after Disinfection? How Many Times? ACS Nano 2020, 14 (5), 6348–6356. [PubMed: 32368894]

(19). Zulauf KE; Green AB; Ba ANN; Jagdish T; Reif D; Seeley R; Dale A; Kirby JE Microwave-Generated Steam Decontamination of N95 Respirators Utilizing Universally Accessible Materials. mBio 2020, 11 (3), e00997–20. [PubMed: 32587063]

(20). Pascoe M; Robertson A; Crayford A; Durand E; Steer J; Castelli A; Wesgate R; Evans S; Porch A; Maillard J Dry heat and microwave-generated steam protocols for the rapid decontamination of respiratory personal protective equipment in response to COVID-19-related shortages. Journal of Hospital Infection 2020, 106 (1), 10–19. [PubMed: 32652212]

(21). Xiang Y; Song Q; Gu W Decontamination of surgical face masks and N95 respirators by dry heat pasteurization for one hour at 70 C. American journal of infection control 2020, 48 (8), 880–882. [PubMed: 32479844]

(22). Fischer RJ; Morris DH; Van Doremalen N; Sarchette S; Matson MJ; Bushmaker T; Yinda CK; Seifert SN; Gamble A; Williamson BN; Judson SD; De Wit E; Lloyd-Smith JO; Munster

VJ Effectiveness of N95 Respirator Decontamination and Reuse against SARS-CoV-2 Virus. Emerging Infectious Diseases 2020, 26 (9), 2253–2255. [PubMed: 32491983]

(23). Anderegg L; Meisenhelder C; Ngooi CO; Liao L; Xiao W; Chu S; Cui Y; Doyle JM A scalable method of applying heat and humidity for decontamination of N95 respirators during the COVID-19 crisis. PloS one 2020, 15 (7), No. e0234851. [PubMed: 32609741]

(24). Campos RK; Jin J; Rafael GH; Zhao M; Liao L; Simmons G; Chu S; Weaver SC; Chiu W; Cui Y Decontamination of SARS-CoV-2 and Other RNA Viruses from N95 Level Meltblown Polypropylene Fabric Using Heat under Different Humidities. ACS Nano 2020, 14 (10), 14017–14025. [PubMed: 32955847]

(25). Weaver DT; McElvany BD; Gopalakrishnan V; Card KJ; Crozier D; Dhawan A; Dinh MN; Dolson E; Farrokhian N; Hitomi M; Ho E; Jagdish T; King ES; Cadnum JL; Donskey CJ; Krishnan N; Kuzmin G; Li J; Maltas J; Mo J; Pelesko J; Scarborough JA; Sedor G; Tian E; An GC; Diehl SA; Scott JG UV decontamination of personal protective equipment with idle laboratory biosafety cabinets during the COVID-19 pandemic. PLoS One 2021, 16 (7), No. e0241734. [PubMed: 34310599]

(26). Wang D; Sun B-C; Wang J-X; Zhou Y-Y; Chen Z-W; Fang Y; Yue W-H; Liu S-M; Liu K-Y; Zeng X-F; et al. Can masks be reused after hot water decontamination during the COVID-19 pandemic? Engineering 2020, 6 (10), 1115–1121. [PubMed: 32837748]

(27). Schwan J; Alva TR; Nava G; Rodriguez CB; Dunn ZS; Chartron JW; Morgan J; Wang P; Mangolini L Efficient facemask decontamination via forced ozone convection. Sci. Rep 2021, 11, 12263. [PubMed: 34112900]

(28). Reed NG The history of ultraviolet germicidal irradiation for air disinfection. Public health reports 2010, 125 (1), 15–27.

(29). Mills D; Harnish DA; Lawrence C; Sandoval-Powers M; Heimbuch BK Ultraviolet germicidal irradiation of influenza-contaminated N95 filtering facepiece respirators. American journal of infection control 2018, 46 (7), e49–e55. [PubMed: 29678452]

(30). Ludwig-Begall L; Wielick C; Dams L; Nauwynck H; Demeuldre P-F; Napp A; Laperre J; Haubruge E; Thiry E The use of germicidal ultraviolet light, vaporized hydrogen peroxide and dry heat to decontaminate face masks and filtering respirators contaminated with a SARS-CoV-2 surrogate virus. Journal of Hospital Infection 2020, 106 (3), 577–584. [PubMed: 32889029]

(31). Alvarez NT; Noga R; Chae S-R; Sorial GA; Ryu H; Shanov V Heatable carbon nanotube composite membranes for sustainable recovery from biofouling. Biofouling 2017, 33 (10), 847–854. [PubMed: 28994321]

(32). Oh Y; Noga R; Shanov V; Ryu H; Chandra H; Yadav B; Yadav J; Chae S Electrically heatable carbon nanotube point-of-use filters for effective separation and in-situ inactivation of Legionella pneumophila. Chemical Engineering Journal 2019, 366, 21–26. [PubMed: 31275054]

(33). Yang P; Wang X COVID-19: a new challenge for human beings. Cellular & Molecular Immunology 2020, 17 (5), 555–557. [PubMed: 32235915]

(34). Babaahmadi V; Amid H; Naeimirad M; Ramakrishna S Biodegradable and multifunctional surgical face masks: A brief review on demands during COVID-19 pandemic, recent developments, and future perspectives. Sci. Total Environ 2021, 798, No. 149233. [PubMed: 34329934]

(35). Larsen GS; Cheng Y; Daemen LL; Lamichhane TN; Hensley DK; Hong K; Meyer HM; Monaco SJ; Levine AM; Lee RJ; Betters E; Sitzlar K; Heineman J; West J; Lloyd P; Kunc V; Love L; Theodore M; Paranthaman MP Polymer, Additives, and Processing Effects on N95 Filter Performance. ACS Applied Polymer Materials 2021, 3 (2), 1022–1031. [PubMed: 37556233]

(36). Xu EG; Ren ZJ Preventing masks from becoming the next plastic problem. Front. Environ. Sci. Eng 2021, 15 (6), 125. [PubMed: 33686360]

(37). Dudchenko AV; Chen C; Cardenas A; Rolf J; Jassby D Frequency-dependent stability of CNT Joule heaters in ionizable media and desalination processes. Nature Nanotechnol. 2017, 12 (6), 557–563. [PubMed: 28553963]

(38). Zuo K; Wang W; Deshmukh A; Jia S; Guo H; Xin R; Elimelech M; Ajayan PM; Lou J; Li Q Multifunctional nanocoated membranes for high-rate electrothermal desalination of hypersaline waters. Nature Nanotechnol. 2020, 15 (12), 1025–1032. [PubMed: 33106641]

(39). Lindsley WG; Martin SB Jr; Thewlis RE; Sarkisian K; Nwoko JO; Mead KR; Noti JD Effects of ultraviolet germicidal irradiation (UVGI) on N95 respirator filtration performance and structural integrity. Journal of occupational and environmental hygiene 2015, 12 (8), 509–517. [PubMed: 25806411]

(40). Ju JT; Boisvert LN; Zuo YY Face masks against COVID-19: Standards, efficacy, testing and decontamination methods. Adv. Colloid Interface Sci 2021, 292, No. 102435. [PubMed: 33971389]

(41). Polkinghorne A; Branley J Evidence for decontamination of single-use filtering facepiece respirators. Journal of Hospital Infection 2020, 105 (4), 663–669. [PubMed: 32473179]

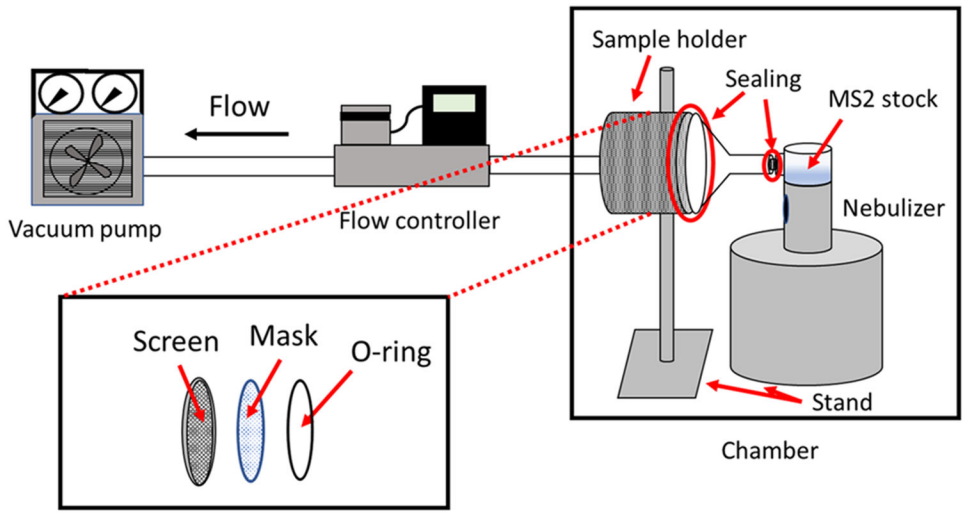

Figure 1.
Schematic illustration of the vacuum system used to generate aerosolized MS2 bacteriophages.

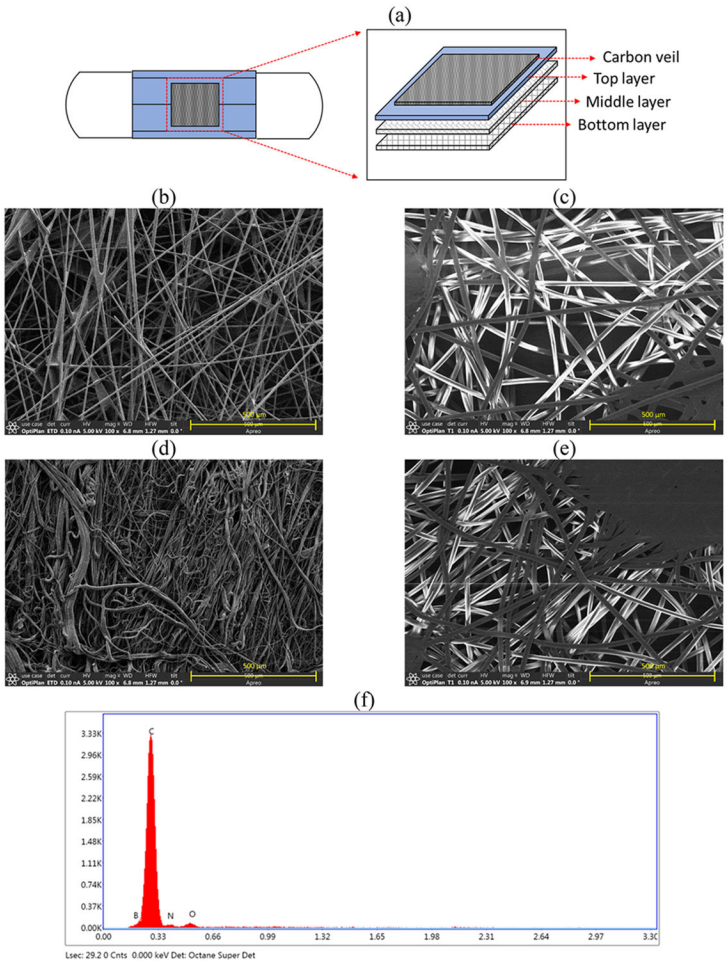

Figure 2.

SEM-EDX of an ASTM Level 3 face mask and a carbon veil (CV) sheet: (a) schematic of an ASTM Level 3 face mask with an electrically heatable CV layer; (b) CV layer; (c) top layer of the ASTM Level 3 face mask; (d) middle layer of the ASTM Level 3 face mask; (e) bottom layer of the ASTM Level 3 face mask; and (f) EDX analysis data of a CV layer.

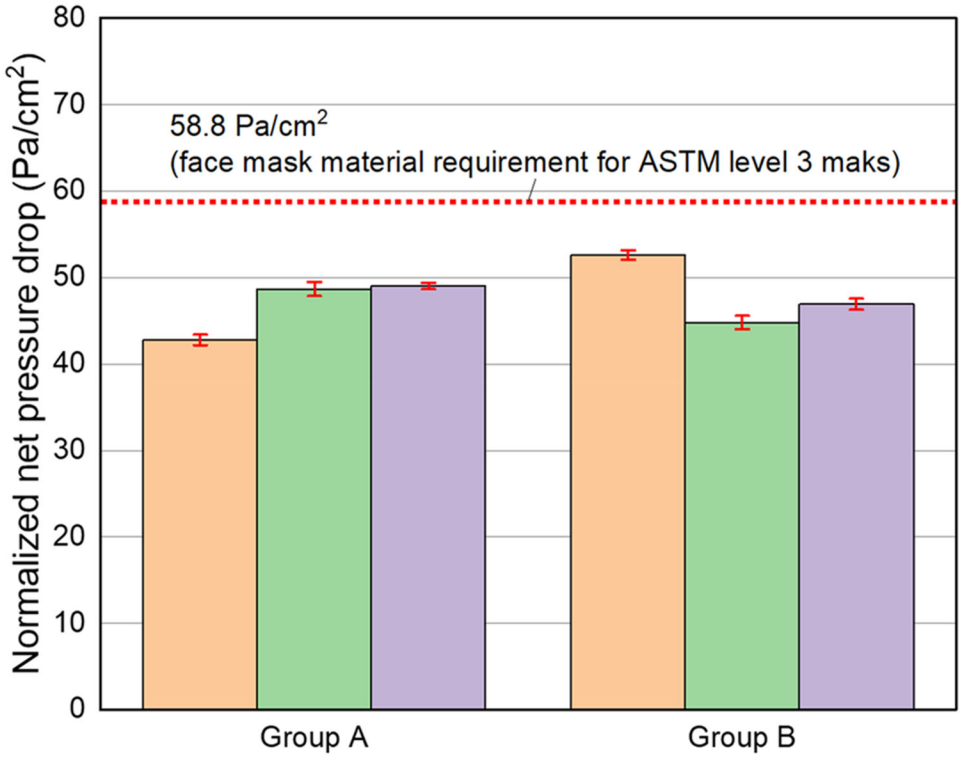

Figure 3.

Normalized net pressure drops using commercial ASTM Level 3 masks without/with a CV layer. Effective surface area: 3.8 cm^2. Air flow = 6.2 L/min. Group A: ASTM Level 3 mask. Group B: ASTM Level 3 mask with a CV layer. Each error bar means ± 95% confidence interval for a normalized net pressure drop. All measurements were performed in triplicate.

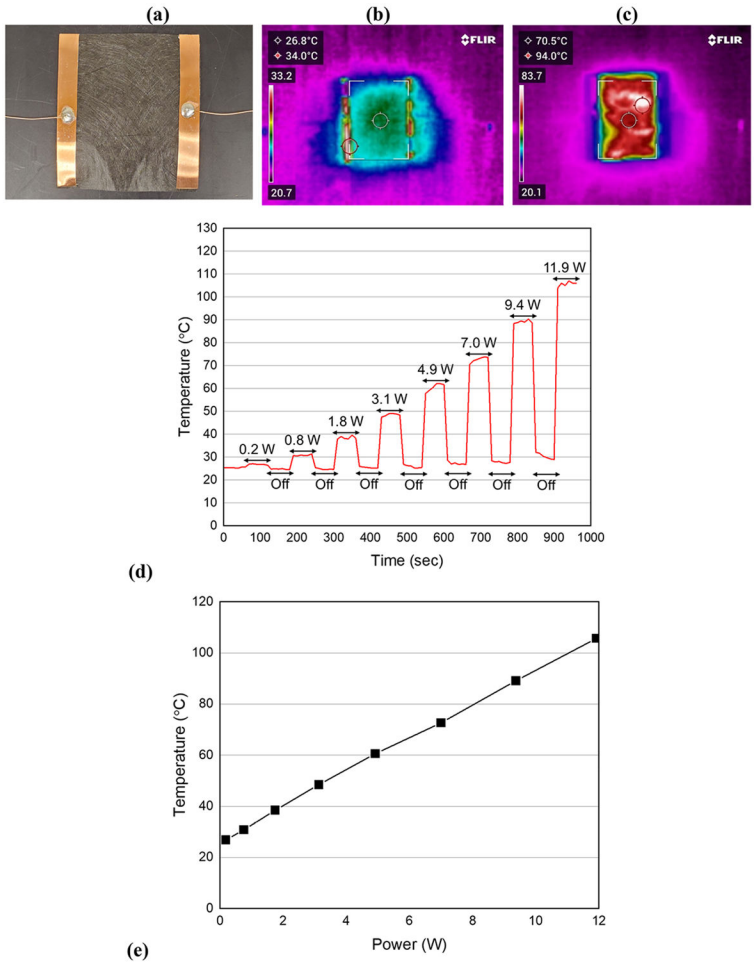

Figure 4.

Performance of Joule heating by using a CV layer in air. An effective heating area of the heater was 41.25 cm^2 (5.5 × 7.5 cm). (a) Electrically heatable CV layer. (b) IR image at time = 660 s (applied DC power = 0 W). (c) IR image at time = 670 s (applied DC power = 7 W). (d) Average surface temperature of the CV when increasing the applied DC power in a pulsed manner (on/off). (e) Correlation between the average surface temperature of the CV and electrical power.

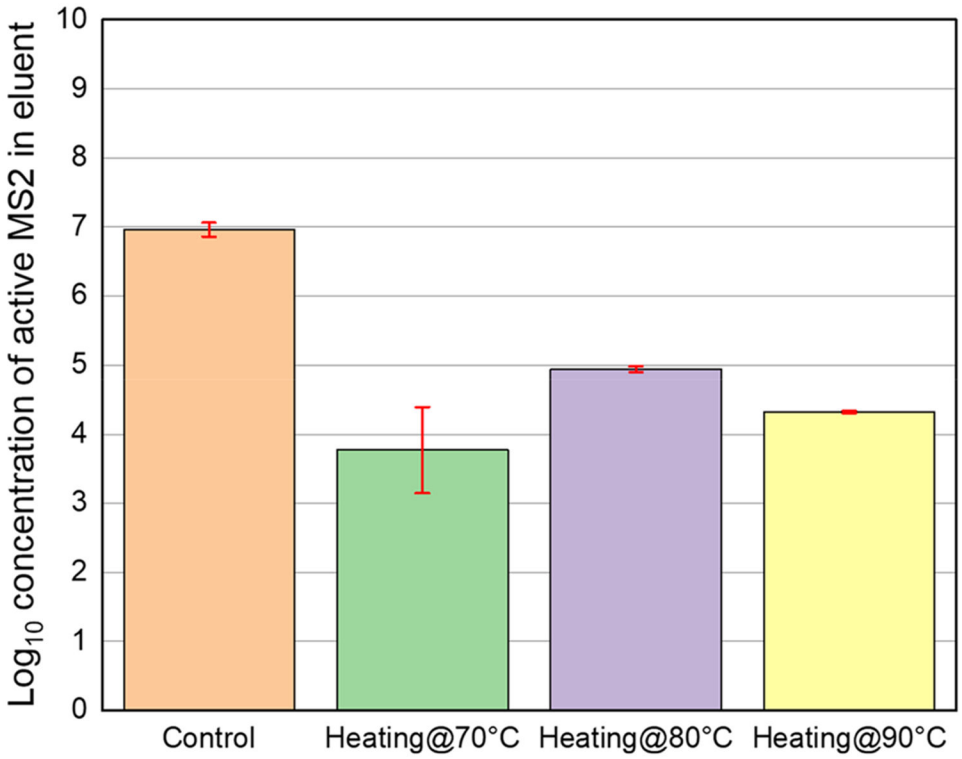

Figure 5.

Log-concentration of active MS2 in eluant. Control: sample without Joule heating, Heating@70 °C: Joule heating at 70 °C. Heating@80 °C: Joule heating at 80 °C. Heating at 90 °C: Joule heating at 90 °C. The Joule heating was conducted for 5 min. Each error bar means ± 95% confidence interval for log-concentration of active MS2. All experiments were duplicated.

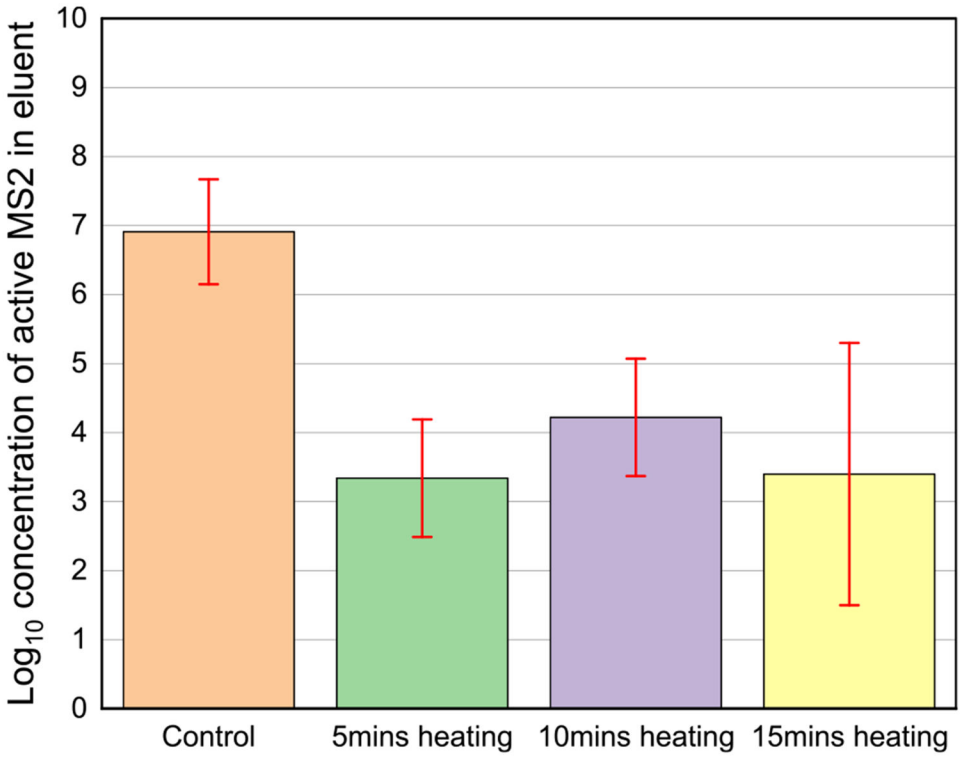

Figure 6.

Log-concentration of active MS2 in eluant. Control: sample without Joule heating, 5min heating: Joule heating conducted for 5 min. 10min heating: Joule heating conducted for 10 min. 15min heating: Joule heating conducted for 15 min. The Joule heating using the CV layer was conducted at 70 °C. Each error bar means ± 95% confidence interval. All experiments were duplicated.

Table 1.

Properties of the ASTM Level 3 Face Mask and the CV Layer

parameter	face mask	CV
areal density (g/m^2)	85.0 ± 2.67^b	16.95^a
thickness (mm)	0.282 ± 0.0183^b	0.127^a
material	polypropylene	polyacrylonitrile (PAN) carbon fiber and polyester binder[a]
bacterial filtration efficiency (%)	$>98^a$	not available
particle filtration efficiency (%)	$>98^a$	not available
breathability (Pa/cm^2)	$<49^a$	0.1 ± 0.03^b
manufacturer	Vaxxen Laboratories, USA	ACP composites, USA

[a]Details provided by the manufacturers.

[b]To determine actual thickness for face masks, measurements were taken using an electronic outside micrometer (Schut Geometrical Metrology).